

Available online at www.sciencedirect.com

jmr&t
Journal of Materials Research and Technology
www.jmrt.com.br



Original Article

Effect of Mg addition on LaMnO₃ ceramic system

García Iván Supelano^{a,*}, Aura J. Barón-González^a, Armando Sarmiento Santos^a, César Ortiz^a, Julieth A. Mejía Gómez^b, Carlos A. Parra Vargas^a

^a Universidad Pedagógica y Tecnológica de Colombia, Tunja 150003, Colombia

^b Universidad Antonio Nariño, Boyacá 150003, Colombia

ARTICLE INFO

Article history:

Received 7 October 2016

Accepted 28 May 2017

Available online 26 August 2017

Keywords:

Magnetic materials

Doped LaMnO₃

ABSTRACT

In the present work we report the synthesis of La_{1-x}Mg_xMnO₃ (with x=0.10, 0.25, and 0.50) polycrystalline samples based on LaMnO₃ (LMO) antiferromagnetic with low Neel temperature and insulating behavior. Structure was analyzed by Rietveld fitting of XRD patterns at room temperature by FullProf software, these show that La_{1-x}Mg_xMnO₃ (x=0.10, 0.25, 0.50) samples crystallize in the space group R-3c. Magnetic and electrical measurements exhibits ferromagnetic and semiconductor like behavior. A decreases of T_C is observed when x doping value increases.

© 2017 Brazilian Metallurgical, Materials and Mining Association. Published by Elsevier Editora Ltda. This is an open access article under the CC BY-NC-ND license (<http://creativecommons.org/licenses/by-nc-nd/4.0/>).

1. Introduction

LaMnO₃ (LMO) is an inorganic compound with perovskite structure. It is an A-type antiferromagnetic insulator with a low Neel temperature [1–4]. Depending on the synthesis process, LMO samples can be obtained as thin films [5], monocrystals [3,6] and polycrystalline powders [7]. To prepare stoichiometric LMO ceramics, the synthesis has to be carried out in low partial pressures of oxygen. In contrast, non-stoichiometric LaMnO_{3+d} is obtained when the production is made in air [8].

The presence of Mn⁴⁺ influences the structural and magnetic behavior of LMO samples. For instance, it has been

reported that for 12% of Mn⁴⁺ content, the structure is orthorhombic with antiferromagnetic ordering. Whereas for higher Mn⁴⁺ content, the structure is rhombohedral or cubic exhibiting ferromagnetism [9].

Partial substitution of lanthanum ions [3,9,10] or Mn ions [11,12] has an effect on the physical properties of LaMnO₃ such as structural changes and Mn⁴⁺/Mn³⁺ ratio. The last one promotes phenomena such as charge and orbital ordering, which are controlled by interaction between electrons from e_g and t_{2g} levels [13].

The aim of this paper is to present the results from the production and characterization of polycrystalline La_{1-x}Mg_xMnO₃ (x=0.10, 0.25, 0.50).

* Corresponding author.

E-mail: ivan.supelano@uptc.edu.co (G.I. Supelano).

<https://doi.org/10.1016/j.jmrt.2017.05.012>

2238-7854/© 2017 Brazilian Metallurgical, Materials and Mining Association. Published by Elsevier Editora Ltda. This is an open access article under the CC BY-NC-ND license (<http://creativecommons.org/licenses/by-nc-nd/4.0/>).

2. Experimental

Polycrystalline $\text{La}_{1-x}\text{Mg}_x\text{MnO}_3$ ($x=0.10, 0.25, 0.50$) samples were prepared by the usual solid state reaction method from a stoichiometric mixture of high purity La_2O_3 (99.99%), MgO (99.995%) and MnO_2 (99.99%) in air at sintering temperature of 1150°C by 24 h at $2.5^\circ\text{C}/\text{min}$ of heating and cooling rate. X-ray powder diffraction (XRD) data were collected on PANalytical X'Pert's X ray diffractometer with $\text{K}_{\alpha\text{-Cu}}$ radiation at room temperature. XRD patterns were studied by Rietveld method with FullProf software. Surface was analyzed by scanning electron microscopy (SEM) with JEOL JSM-6490LV microscope and elemental analysis (EDS) with EDS Inca Energy 250 analyzer. Magnetization measurements were performed in vibrating magnetometer Versalab and Physical Property Measurements System (PPMS) of Quantum-Design. Electrical resistance measurements were performed with PPMS by using the standard 4-probe method.

3. Results and discussion

XRD patterns for $\text{La}_{1-x}\text{Mg}_x\text{MnO}_3$ samples are displayed in Fig. 1(a). Based on these diffraction patterns, it can be observed that lanthanum manganites Mg-doped range from 0.25 to 0.50 exhibit the same phase. However, for the samples with $x=0.25$ and 0.5, additional reflections at $2\theta=35.57^\circ$ and $2\theta=36.37^\circ$

are detected. This corresponds to a secondary phase Mn_3O_4 (peaks marked as Δ).

Rietveld analysis (Fig. 1(b-d)) suggests that all the samples crystallize in the rhombohedral $R\bar{3}c$ space group. This result differs from that reported by Zhao et al. [14]. They obtained the $Pbnm$ structure for samples with $x=0.05, 0.10, 0.20, 0.33$ and 0.40 . This difference can be attributed to different conditions of synthesis. The structural parameters of $\text{La}_{1-x}\text{Mg}_x\text{MnO}_3$ ($x=0.10, 0.25, 0.50$) were refined by fitting the XRD patterns using the program FullProf (Table 1). Substitution of La with Mg causes changes in the lattice parameters due to smaller Mg ionic radius than La ionic radius.

Fig. 2 shows the scanning electron micrograph (SEM) of $\text{La}_{1-x}\text{Mg}_x\text{MnO}_3$ ($x=0.10, 0.25, 0.50$) samples. These images show that, there is no significant change in the morphology with increasing Mg concentration in LMO. The grain size distributions for each sample are shown in the insets of Fig. 2. For $x=0.1$ the grain size ranges between 3.23 and $1.83\ \mu\text{m}$, for $x=0.25$ between 2.45 and $1.65\ \mu\text{m}$, and for $x=0.5$ between 1.93 and $1.13\ \mu\text{m}$. Hence, it is concluded that in $\text{La}_{1-x}\text{Mg}_x\text{MnO}_3$ ($x=0.10, 0.25, 0.50$), the Mg substitution at the lanthanum positions induces decreasing of grain size. This result is in agreement with the decreasing of cell volume that is clearly observed from the Rietveld analysis (Table 1). EDS analysis ruled out the presence of other traces elements.

The ZFC-FC $M(T)$ curves of $\text{La}_{1-x}\text{Mg}_x\text{MnO}_3$ ($x=0.10, 0.25, 0.50$) are illustrated in Fig. 3. The plots evidence the ferromagnetic behavior for all the samples. In order to understand the

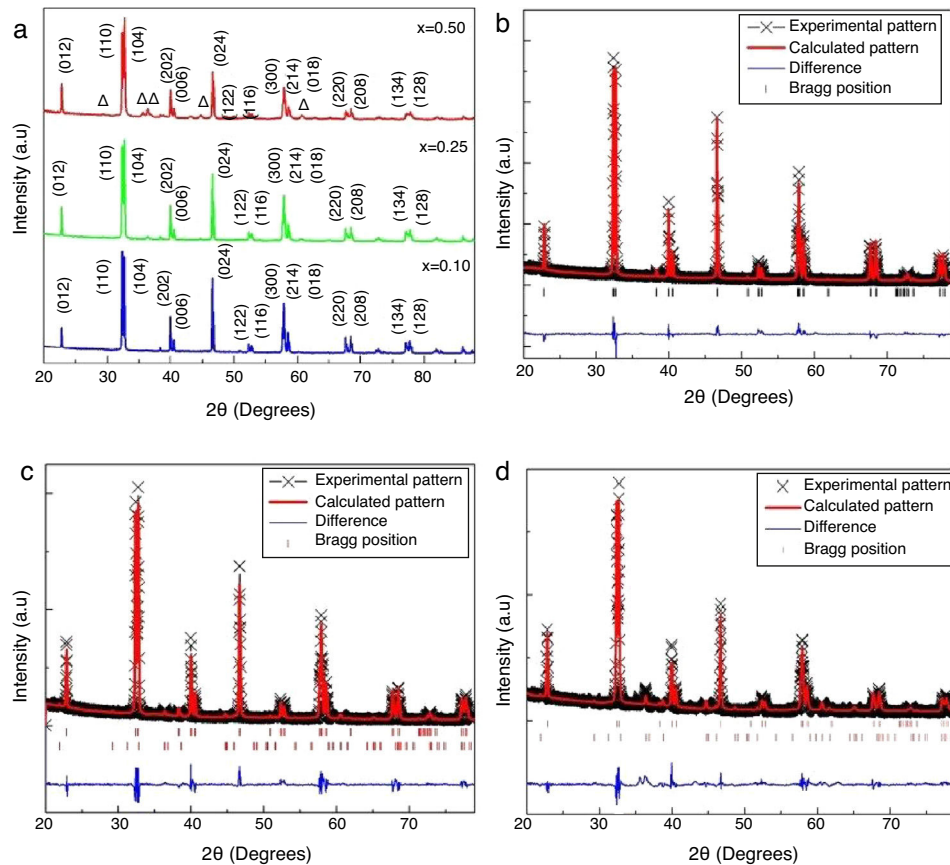
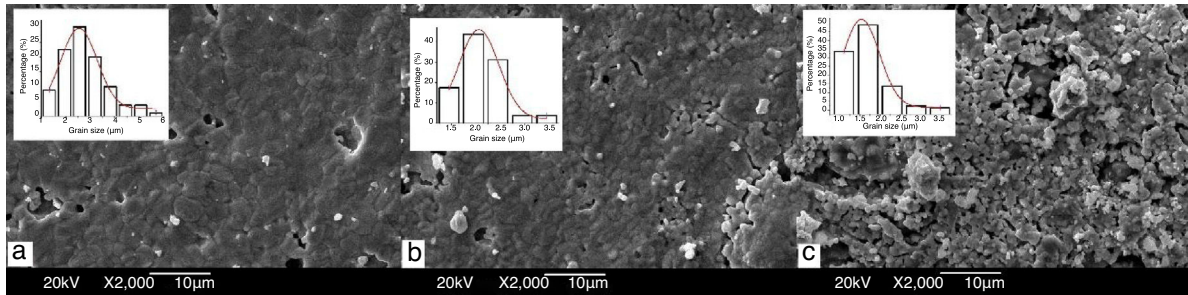


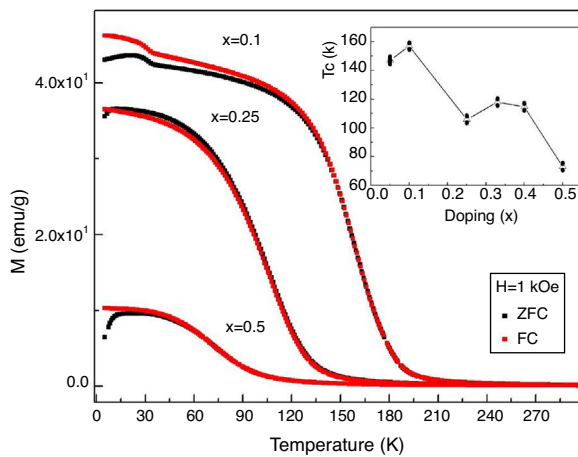
Fig. 1 – (a) XRD patterns of $\text{La}_{1-x}\text{Mg}_x\text{MnO}_3$ system. Rietveld analysis for (b) $\text{La}_{0.9}\text{Mg}_{0.1}\text{MnO}_3$, (c) $\text{La}_{0.75}\text{Mg}_{0.25}\text{MnO}_3$ and (d) $\text{La}_{0.5}\text{Mg}_{0.5}\text{MnO}_3$ sample at 300 K.

Table 1 – Structural details of $\text{La}_{1-x}\text{Mg}_x\text{MnO}_3$ obtained by Rietveld refinement of DRX. La/Mg occupy 6a Wyckoff position ($0\ 0\ \frac{1}{4}$), Mn occupy 6b ($0\ 0\ 0$) and O occupy 18e ($x\ 0\ \frac{3}{4}$).

	$\text{La}_{0.9}\text{Mg}_{0.1}\text{MnO}_3$	$\text{La}_{0.75}\text{Mg}_{0.25}\text{MnO}_3$	$\text{La}_{0.5}\text{Mg}_{0.5}\text{MnO}_3$
Lattice parameters			
$a = b$ (Å)	5.534(5)	5.529(4)	5.526(1)
c (Å)	13.354(5)	13.345(3)	13.339(9)
Statistical parameters of fitting			
R_{Bragg} (%)	6.28	7.27	6.12
R_f (%)	4.20	5.34	6.04
Atomic positions			
O x	0.44699	0.43746	0.44501
Cell volume V (Å³)			
	354.267	353.351	352.784
	162.8(6)	Mn–O–Mn BOND ANGLE (°)	163.9(9)
	1.969(6)	Mn–O BOND LENGTH (Å)	1.964(6)

**Fig. 2 – SEM micrographs of (a) $\text{La}_{0.9}\text{Mg}_{0.1}\text{MnO}_3$, (b) $\text{La}_{0.75}\text{Mg}_{0.25}\text{MnO}_3$ and (c) $\text{La}_{0.5}\text{Mg}_{0.5}\text{MnO}_3$.****Table 2 – Data of magnetization: Curie temperature (T_C), remnant magnetization (M_r), coercive field (H_c) and saturation magnetization (M_s).**

Doping x	T_C (K)	M_r (emu/g) at 5 K	H_c (Oe) at 5 K	M_s (emu/g) at 5 K
0.1	157	1.53	15	79.35
0.25	106	5.86	43	49.59
0.5	73	3.05	137	20.88

**Fig. 3 – Curves ZFC-FC for the $\text{La}_{1-x}\text{Mg}_x\text{MnO}_3$ ($x = 0.1, 0.25$ and 0.5) samples. Inset displays the T_C obtained for the three samples produced in this work plus data for $x = 0.05$ [2], 0.33 [14], 0.40 [14].**

influence of Mg doping at La site, the Curie temperature (T_C) change of the samples (T_C determined by the minimum value of the derivative of magnetization as a function of the temperature in the ZFC curve) is shown in the inset of Fig. 3. The values of T_C were found to decrease with Mg content.

The M vs H hysteresis plot of $\text{La}_{1-x}\text{Mg}_x\text{MnO}_3$ ($x = 0.10, 0.25, 0.50$) at 5 and 50 K (Fig. 4(a and b)) indicate ferromagnetic behavior at low temperatures. Whereas at 300 K (Fig. 4(c)) the behavior is paramagnetic.

$\text{La}_{1-x}(\text{Ca}, \text{Sr})_x\text{MnO}_3$ samples exhibit similar behavior [9]. In this work, the content of Mn^{4+} increases as x value increases. Mn–O–Mn bond angle values were found to be 164° approximately. Mn–O bond length values range between 1.92 \AA and 1.96 \AA . Furthermore, there is colossal magnetoresistance (CMR) which is observed only for values of Mn–O bond length below 1.97 \AA . In our study, Mn–O–Mn bond angle values lie between $162.8(6)^\circ$ and $164.2(5)^\circ$. The values of Mn–O bond length are around $1.969(6) \text{ \AA}$. However, CMR was not observed.

Log R is plotted in Fig. 5 as a function of the inverse of the absolute temperature. Samples with $x = 0.10, 0.25$ and 0.50

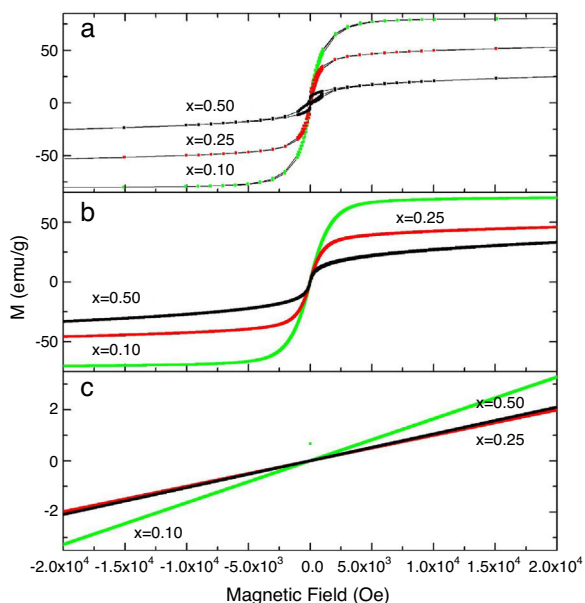


Fig. 4 – Curves M vs H for $\text{La}_{1-x}\text{Mg}_x\text{MnO}_3$ ($x = 0.1, 0.25, 0.5$) samples measured with: (a) PPMS system to 5 K, (b) Versalab system to 50 K and (c) VersaLab system to 300 K.

present a linear behavior, first and second exhibit an inflection at 139 K and 197 K, above T_C . It suggests that samples have a normal semiconductor behavior. Semiconducting behavior also occurs in the sample with $x = 0.05$ [2]. Inset in Fig. 5 shows electrical resistance as a function of the temperature, at applied field of $H = 0$, and $H = 1$ kOe. For sample with $x = 0.10$, resistance increases while the temperature decreases, there is no evidence of magnetoresistance. A similar behavior was found in the other samples.

For this system, based on LMO, the results suggest that previously values of Mn–O–Mn bond angles and Mn–O bond lengths are the reason why the $\text{La}_{1-x}\text{Mg}_x\text{MnO}_3$ ($x = 0.10$,

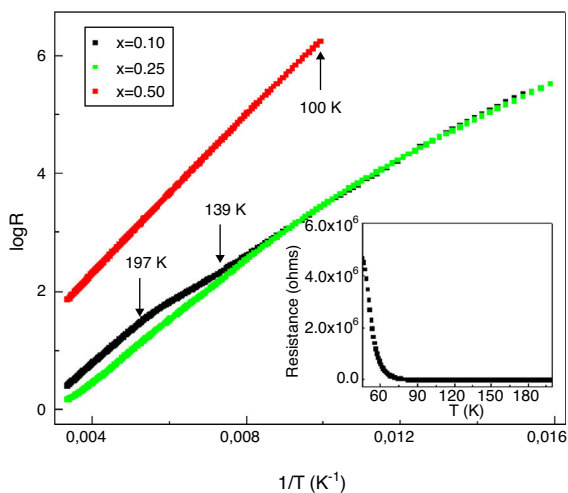


Fig. 5 – Electrical resistance logarithm as a function of the inverse of temperature for $\text{La}_{1-x}\text{Mg}_x\text{MnO}_3$ ($x = 0.1, 0.25, 0.5$) samples. Inset: electrical resistance as a function of temperature for the $\text{La}_{0.9}\text{Mg}_{0.1}\text{MnO}_3$ sample.

0.25, and 0.50) system present ferromagnetism and does not present CMR.

Comparing the present results with those reported by Zhao et al. [14], the T_C obtained is in the same order of magnitude, which permitted to conclude that the better doping value of x is around 0.1. Table 2 listed the values of T_C .

4. Conclusions

Polycrystalline $\text{La}_{1-x}\text{Mg}_x\text{MnO}_3$ ($x = 0.10, 0.25, 0.50$) samples were synthesized by solid state reaction method. The system crystallize in rhombohedral structure (R-3c) at room temperature. The inclusion of Mg in the system, induce interactions which arise the ferromagnetic phase at low temperature. The system present a decrease of T_C when the doping increases. The electrical Response have semiconductor behavior, in which the resistance is proportional the inverse of the temperature. Results suggest that this behavior is due to the strong influence of Mn–O–Mn bond angles and Mn–O bond lengths values.

Conflicts of interest

The authors declare no conflicts of interest.

Acknowledgments

To Institut de Ciència de Materials de Barcelona (CSIC), Dr. Carlos Frontera and Dr. Bernat Bozzo. This work was supported by the Gobernación de Boyacá (N° 733 Colciencias).

REFERENCES

- [1] Wenwei W, Jinchao C, Xuehang W, Sen L, Kaituo W, Lin T. Nanocrystalline LaMnO_3 preparation and kinetics of crystallization process. *Adv Powder Technol* 2013;24:154–9.
- [2] Zhao J, Song T, Kunkel H, Zhou X, Roshko R, Williams G. $\text{La}_{0.95}\text{Mg}_{0.05}\text{MnO}_3$: an ideal ferromagnetic system? *J Phys: Condens Matter* 2000;12:6903.
- [3] Rodríguez-Carvajal J, Hennion M, Moussa F, Moudén AH, Pinsard L, Revcolevschi A. Neutron-diffraction study of the Jahn-Teller transition in stoichiometric LaMnO_3 . *Phys Rev B* 1998;57(6):3189.
- [4] Zhong-Qin Y, Qiang S, Ling Y, Xi-De X. A discrete variational method study on the electronic structures of CaMnO_3 and LaMnO_3 . *Acta Phys Sin-Ov Ed* 1998;7(11):851.
- [5] Khanduri H, Chandra Dimri M, Vasala S, Leinberg S, Lohmus R, Ashworth TV, et al. Magnetic and structural studies of LaMnO_3 thin films prepared by atomic layer deposition. *J Phys D: Appl Phys* 2013;46:175003.
- [6] Zhou J-S, Goodenough JB. Paramagnetic phase in single-crystal LaMnO_3 . *Phys Rev B* 1500;60(22):2.
- [7] Kitayama K. Phase equilibrium in the system Ln–Mn–O: I. Ln = La at 1100 °C. *J Solid State Chem* 2000;153:336–41.
- [8] Topfer J, Goodenough JB. Charge transport and magnetic properties in perovskites of the system La–Mn–O. *Solid State Ionics* 1997;101:1215.
- [9] Mahendiran R, Tiwary SK, Raychaudhuri AK, Ramakrishnan TV, Mahesh R, Rangavittal N. Structure, electron-transport properties, and giant magnetoresistance of hole-doped LaMnO_3 systems. *Phys Rev B* 1996;53(6):3348.

-
- [10] Raychaudhuri P, Mitra C, Mann PDA, Wirth S. Phase diagram and Hall effect of the electron doped manganite $\text{La}_{1-x}\text{Ce}_x\text{MnO}_3$. *J Appl Phys* 2003;93:8328.
- [11] Hebert S, Martin C, Maignan A, Retoux R, Hervieu M, Nguyen N, et al. Induced ferromagnetism in LaMnO_3 by Mn-site substitution: the major role of Mn mixed valency. *Phys Rev B* 2002;65:104420.
- [12] Hansteen Ole H, Bréard Y, Fjellvåg H, Hauback BC. Divalent manganese in reduced $\text{LaMnO}_{3-\delta}$ effect of oxygen nonstoichiometry on structural and magnetic properties. *Solid State Sci* 2004;6:279.
- [13] Frontera C, García-Muñoz JL, Llobet A, Aranda MAG, Ritter C, Respaud M, et al. Room temperature charge and orbital ordering and phase coexistence in $\text{Bi}_{0.5}\text{Sr}_{0.5}\text{MnO}_3$. *J Phys: Condens Matter* 2001;13:1071.
- [14] Zhao JH, Kunkel HP, Zhou XZ, Williams G. Magnetic and transport properties, and the phase diagram of hole-doped $\text{La}_{1-x}\text{Mg}_x\text{MnO}_3$ ($x \leq 0.4$). *J Phys: Condens Matter* 2001;13:9349.